Cell

A Spatially-Organized Multicellular Innate Immune Response in Lymph Nodes Limits Systemic Pathogen Spread

Wolfgang Kastenmüller,[1,3,*] Parizad Torabi-Parizi,[1,2,3] Naeha Subramanian,[1] Tim Lämmermann,[1] and Ronald N. Germain[1,*]
[1]Lymphocyte Biology Section, Laboratory of Systems Biology, National Institute of Allergy and Infectious Diseases
[2]Critical Care Medicine Department, Clinical Center
National Institutes of Health, Bethesda, MD 20892, USA
[3]These authors contributed equally to this work
*Correspondence: kastenmullerw@mail.nih.gov (W.K.), rgermain@nih.gov (R.N.G.)
http://dx.doi.org/10.1016/j.cell.2012.07.021

SUMMARY

The lymphatic network that transports interstitial fluid and antigens to lymph nodes constitutes a conduit system that can be hijacked by invading pathogens to achieve systemic spread unless dissemination is blocked in the lymph node itself. Here, we show that a network of diverse lymphoid cells (natural killer cells, γδ T cells, natural killer T cells, and innate-like CD8+ T cells) are spatially pre-positioned close to lymphatic sinus-lining sentinel macrophages where they can rapidly and efficiently receive inflammasome-generated IL-18 and additional cytokine signals from the pathogen-sensing phagocytes. This leads to rapid IFNγ secretion by the strategically positioned innate lymphocytes, fostering antimicrobial resistance in the macrophage population. Interference with this innate immune response loop allows systemic spread of lymph-borne bacteria. These findings extend our understanding of the functional significance of cellular positioning and local intercellular communication within lymph nodes while emphasizing the role of these organs as highly active locations of innate host defense.

INTRODUCTION

The circulatory system transports fluids, nutrients, and hematopoietic cells throughout the body. A significant amount of blood fluid constantly transudes into tissues and is brought back to the circulation via lymphatic vessels, specialized capillaries with an open structure that enhances collection of this interstitial fluid (Alitalo, 2011; Swartz, 2001). In the absence of evolved host defense mechanisms, this open structure and the effects of bulk flow into these vessels would allow pathogens that breach epithelial barriers to be readily flushed into the blood circulation and disseminated to distant tissue sites. To prevent this, the lymphatic system is equipped with filter-like structures, lymph nodes (LNs), within which various lymphoid and myeloid cells reside.

Prior studies suggested that myeloid cells in the LNs play a central role in sequestering particulate material as it moves from the afferent lymph into the subcapsular lymph node sinus (Asano et al., 2011; Lämmermann and Sixt, 2008). Recently, electron microscopy along with static section analysis and dynamic fluorescent intravital imaging have provided new insight into the manner in which draining particles are acquired by CD169+ subcapsular sinus (SCS) and medullary macrophages (Carrasco and Batista, 2007; Cinamon et al., 2008; Gonzalez et al., 2010; Junt et al., 2007). These studies have documented the rapid acquisition of viruses and nano-particles by SCS macrophages and the transfer of some undegraded material to subjacent naive follicular B cells.

Although the "flypaper" function of the sinus-lining macrophages in trapping pathogens arriving in the lymph is well accepted, there is little evidence for the operation of a highly organized, multicellular innate host defense response within draining LNs (dLNs) that reduces the risk of trans-nodal pathogen invasion and spread. Most investigators typically view LNs only as sites of production of antigen-specific (adaptive) effector cells that mediate protection after the egress of activated lymphocytes from these secondary lymphoid organs, not as the location of effector responses that actively resist pathogen growth or dissemination in a local manner. Of course, exceptions exist, such as neutrophil influx in response to local *Toxoplasma* invasion (Chtanova et al., 2008) or cytotoxic CD8+ T cell responses operating in LNs to kill HIV-infected CD4+ T cells (Borrow et al., 1997), but this is still within the paradigm that adaptive effectors act mainly in the infected tissue site, here cells resident within the LN itself.

This view of the LN does not explain the local presence of a number of immune cell types that in other tissues have a well-known role in antipathogen defense; this includes natural killer (NK) cells (Shi et al., 2011), natural killer T (NKT) cells (Bendelac et al., 2007), and γδ T cells (Hayday, 2009). Given the evident importance of blocking the spread of lymph-borne

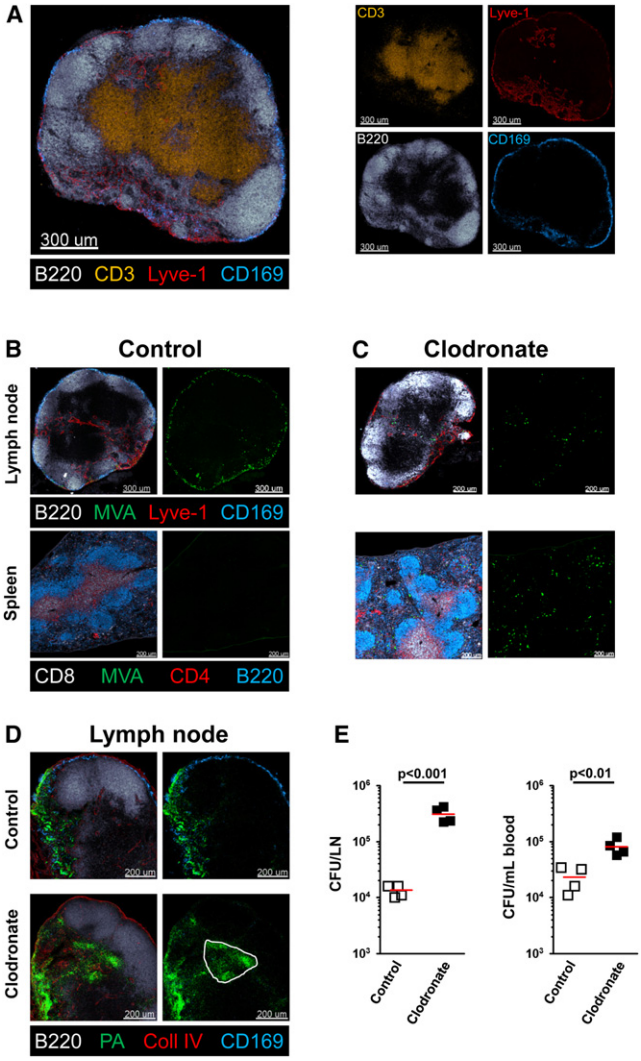

Figure 1. LN Macrophages Prevent Systemic Spread of Pathogens

(A) Confocal immunofluorescence (IF) image showing the basic anatomy of a peripheral LN stained with antibodies to the indicated marker molecules. Colors of the word labels correspond to the colors of the stains here and throughout.

(B and C) Confocal IF of draining LN and spleen 4 hr after s.c. infection with MVA-GFP. Mice were pretreated 7 days before infection by s.c. injection of control (B) or clodronate-containing liposomes (C).

(D and E) Confocal IF of a draining LN (D) and bacterial counts of blood and of LN homogenates (E) 8 hr after s.c. (footpad) infection with PA-GFP. Mice were pretreated 7 days before infection by s.c. (calf) injection of control or clodronate-containing liposomes. Red bars = mean. The experiment is representative of three similar experiments and p values from two-tailed t test are shown (see also Figure S1).

pathogens before they gain access to the blood circulation, it seemed likely to us that these cells might play an active role in providing innate defense within LNs. We were particularly drawn to this concept by two considerations. First, the microbicidal activity of myeloid cells, especially macrophages, is markedly augmented by cytokines produced by lymphoid cells (Benoit et al., 2008; Mantovani et al., 2002). Second, given that the spatial organization of cells within LNs plays a major role in the efficient functioning of the adaptive immune system (Bajénoff et al., 2006b; Cahalan and Parker, 2006; Castellino et al., 2006; Germain et al., 2008; Gretz et al., 1997; Kastenmüller et al., 2010; Okada and Cyster, 2006; Pereira et al., 2010; Sumen et al., 2004), it seemed possible that these numerically small subpopulations might be located anatomically within the node in a specific manner facilitating innate host defense.

Based on these considerations, we undertook a careful examination of whether distinct immune cell populations might be spatially and functionally organized in LNs to facilitate an acute innate immune response that limits systemic pathogen spread. Here we report that this is indeed the case; SCS macrophages orchestrate a complex interplay involving locally prepositioned innate immune lymphocytes as well as recruited neutrophils that provides a rapid and robust response to lymph-borne pathogens, especially bacteria. Interference with this set of reciprocal interactions involving inflammasome activation, IL-1 family member cytokine production, lymphoid cell IFNγ secretion, and activation of the macrophage population, limits the effectiveness of the innate response, allowing deep invasion of the LN by bacteria and systemic spread of these pathogens.

RESULTS

LN Macrophages Are the Site of Initial Infection by Lymph-Borne Virus and Prevent Systemic Spread

T cells reside in the paracortex of the lymph node, surrounded by B cells that are organized into primary follicles subjacent to the subcapsular sinus that receives incoming lymph (Lämmermann and Sixt, 2008). Macrophages are positioned within or in close physical proximity to the cortical and medullary sinuses into which lymph drains (Figures 1A and S1A available online). Studies with VSV showed that many viral particles associate with SCS macrophages, and these are also the primary targets of replication-deficient vaccinia virus (modified vaccinia Ankara [MVA]) administered into the skin (Junt et al., 2007; Norbury et al., 2002). Consistent with this prior knowledge, subcutaneous (s.c.) footpad injection of a green fluorescent protein (GFP)-expressing variant of MVA revealed infection of many of these macrophages by 4 hr postadministration (Figure 1B). Importantly, no GFP-positive cells could be found in the spleen after such local infection, indicating that the virus did not spread systemically after being carried to the LN via the lymph (Figure 1B). In contrast, after local depletion of these macrophages in the draining lymph node (dLN) using clodronate-loaded liposomes (Van Rooijen and Sanders, 1994), only a few virally-infected GFP-positive cells could be found in the lymph node, but there were now many GFP-positive infected cells in the spleen (Figure 1C). This demonstrates that in the absence of effective viral capture by SCS macrophages systemic spread ensues. However, host-adapted poxvirus preferentially replicate in macrophages (Senkevich et al., 1995), so this apparent filtering effect might actually represent loss of the preferred cellular target and not a general pathogen capture mechanism involving the SCS phagocytes.

Role of SCS Macrophages in Preventing Spread of Extracellular Bacteria

SCS macrophages have a propensity to capture particulate material arriving in the afferent lymph (Carrasco and Batista, 2007; Cinamon et al., 2008; Junt et al., 2007), so we hypothesized that these myeloid cells would be crucial to preventing systemic spread of bacteria. To avoid the complication of the SCS macrophages acting as the major host cell for invading organisms, we repeated the depletion studies using an extracellular bacterium (*Pseudomonas aeruginosa* [PA]) that does not target macrophages for replication. PA is a gram-negative bacterium that causes medically important pulmonary and skin infections, the latter particularly after burn injuries (Bodey et al., 1983), and importantly does not actively infect macrophages. As seen with MVA infection, after s.c. footpad infection with PA-expressing GFP (PA-GFP) bacteria were found 8 hr postinfection in the cortical and particularly the medullary sinuses of the skin dLN (Figure 1D). In contrast, after local clodronate depletion of macrophages, PA-GFP infiltrated the LN parenchyma (Figure 1D). We specifically employed two separate injections sites for clodronate (calf) and bacterial challenge (footpad) to eliminate the possibility that of skin-resident macrophages were playing an essential role in bacterial elimination in this experimental set-up. To quantify the local infection in the dLN and gain information about possible systemic spread, we cultured LN suspensions and blood of PA-infected mice that had been locally depleted of macrophages in the dLN (but not the spleen; Figure S1B) or treated with empty liposomes. We found a nearly 10-fold increase in the local and systemic bacterial loads in macrophage-depleted mice (Figure 1E), indicating that the macrophage layer is essential to limiting local replication and systemic spread of lymph-borne pathogens.

Rapid Innate IFNγ Production by LN Resident Lymphoid Cells upon Skin Infection

The bactericidal capacity of macrophages is greatly augmented by co-operative interactions with lymphoid cells (Mantovani et al., 2002). Therefore, we asked whether the latter are also involved in an acute response to invading organisms. Because lymphoid and myeloid cells communicate via cytokines to enhance host defense (Dayer, 2003), we screened the lymphocyte population of LN draining the site of PA infection for the production of various cytokines by direct ex vivo examination without restimulation. CD44 expression was employed as a broad marker of lymphoid cells that may have an effector phenotype (DeGrendele et al., 1997). Strikingly, 4 hr after s.c. footpad infection with PA, we observed a significant number of IFNγ-producing lymphoid cells (Figure 2A). Macrophage depletion reduced the frequency of IFNγ-producing cells by 3-fold and the absolute amount of IFNγ produced per cell by about 2-fold, based on mean fluorescent intensity (Figure 2A and 2B). These data indicate that lymph node macrophages have a central role in the initiation of an innate immune response involving lymphoid cells in the dLN. The IFNγ-producing lymphoid cell population was detectable as early as 2 hr after infection, with the response plateauing at around 3 to 4 hr (Figure 2C), which is much too rapid to be part of an adaptive immune response. The conclusion that what we observe is an innate rather than an antigen-specific adaptive response is consistent with the finding that although the absolute frequency of such IFNγ-producing lymphoid cells is low (~0.5% of all lymphocytes in the dLN); this represents responses that are nearly 15% of the $CD44^{hi}$ subpopulation, a fraction much larger than would be expected for a primary specific adaptive response to a single organism.

The $CD44^{hi}$IFNγ+ population was further characterized phenotypically and found to be composed of approximately 15% NK cells, 20% γδ T cells plus NKT cells, and, surprisingly, about 65% αβ TCR CD8+ T cells (Figure 2D). To better define the IFNγ+ CD8+ population, we performed the PA infection experiment in germ-free mice (lacking classical memory CD8+ T cells to foreign antigens) and SAP KO mice (lacking NKT cells) and found that although the IFNγ response was reduced (Figure 2E), the relative contribution of CD8+ T cells to the total IFNγ response was not significantly altered (Figure S2). These data indicate that the CD8+ effector T cells with innate-like properties are not antigen-specific for PA or cross-reactive with these bacteria due to prior microbial experience, nor do they represent the recently described NKT- and IL-4-dependent innate CD8+ T cells found in Balb/c mice (Weinreich et al., 2010). Surprisingly, even MHCI KO and β2m KO mice contained an innate-like CD8+ T cell population that contributed significantly to the total IFNγ response elicited in the dLN after bacterial challenge (Figure 2F). The CD8+ T cells responding in β2m KO animals and partially those responding in MHCI KO animals, however, were not classical CD8+ T cells, as they expressed a γδ TCR instead of an αβ TCR (Figure 2G). Taken together, these data show that macrophages regulate a rapid cytokine response involving multiple innate effector lymphoid cells in the dLN. We further identify a previously unrecognized, noncognate, innate-like subpopulation of αβ CD8+ T cells as an important component of the early acute immune response to bacterial infections in the LN.

Requirement for IL-18 and a Second Signal in the Innate IFNγ Response in Draining LNs

Having established a functional connection between LN-resident macrophages and various lymphocyte subsets, we wanted to gain further mechanistic insight into how macrophages activated this diverse group of innate effector cells and whether the acute IFNγ response played a role in limiting systemic spread of lymph-borne bacteria. Given the variety of receptors expressed by NKT, γδ T cells, NK cells, and innate-like CD8+ T cells, cytokine-driven activation seemed a likely possibility for the mode of communication between macrophages detecting initial pathogen arrival via the lymph and these cytokine-producing lymphoid cells. Previous studies have reported that combinatorial cytokine signals can evoke effector cytokine responses from effector T cells in the absence of antigen receptor (TCR) signaling (Guo et al., 2009; Robinson et al., 1997; Yang et al., 2001). Although an obvious candidate, IL-12 was not required to induce an IFNγ response upon PA infection (Figure 3A). In contrast, IL-18 was required for this response. Importantly, IL-18 KO mice did not show a fundamental developmental defect in the various effector cells, as the IFNγ response in all $CD44^{hi}$ subsets of IL-18 KO mice could be rescued by

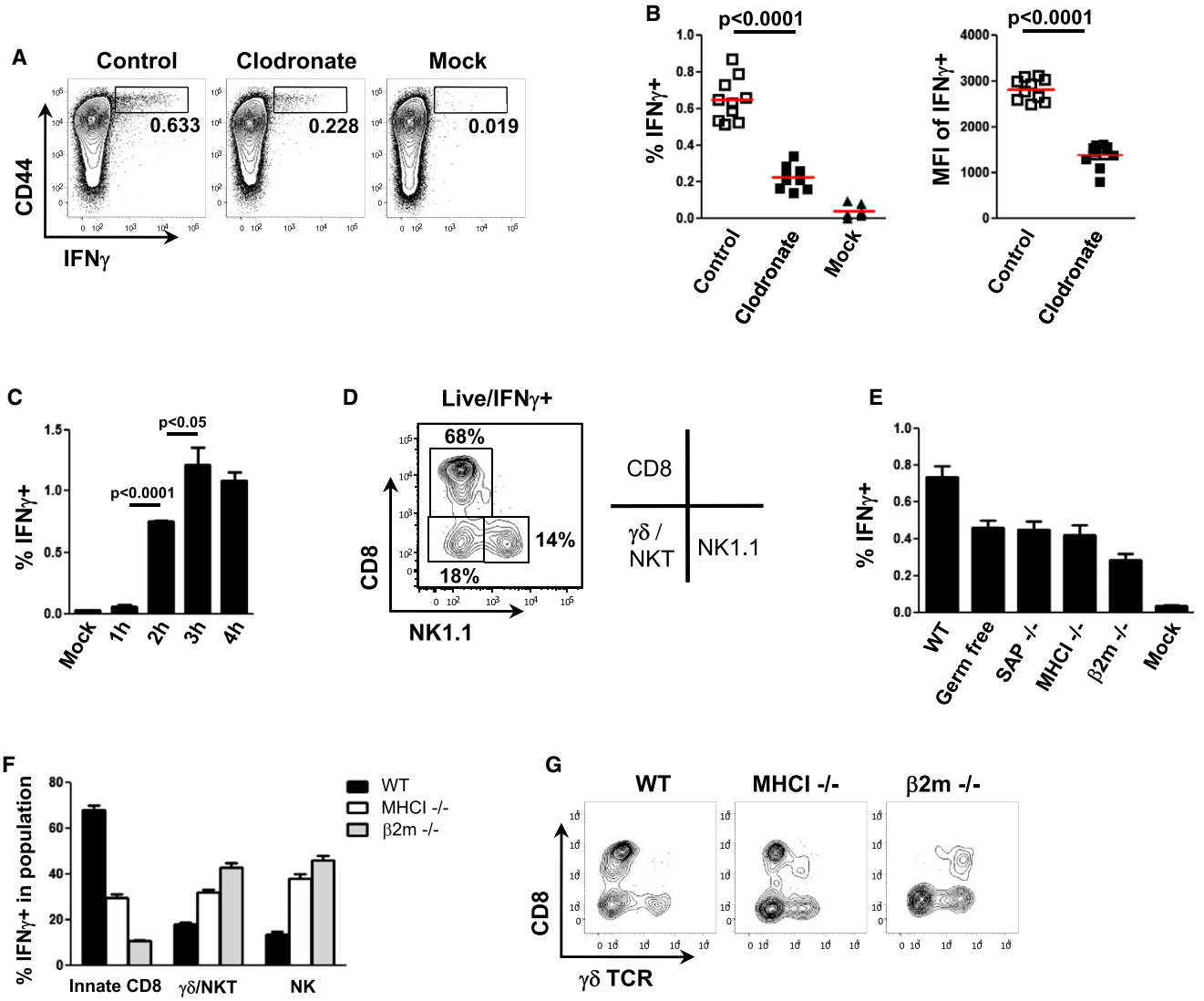

Figure 2. Macrophages Orchestrate an IFNγ Response by Activating Various Innate Effector Cells in the LN

Flow cytometric analysis of cells from a draining LN 4 hr after s.c. infection with PA-GFP. WT mice were pretreated with control or clodronate-containing liposomes 7 days before infection.

(A–F) Analysis of intracellular IFNγ production. (A) Representative flow cytometry plots highlighting $CD44^{hi}$ IFNγ-positive cells (boxes); (B) frequency of IFNγ-positive cells (left) and mean fluorescent intensity of the IFNγ signal (right); each dot represents one mouse, red bar is the mean value; (C) kinetic analysis of IFNγ production after PA infection; (D) phenotypes of immune cell subtypes producing IFNγ; (E) comparison of the frequency of IFNγ-producing cells in various gene-deficient or germ-free mice 4 hr after PA infection; (F) comparison of IFNγ-producing immune cell subtypes in WT, MHCI KO, and β2m KO mice.

(G) Representative flow cytometry plots of γδ TCR expression in WT, MHCI KO, and β2m KO mice. Graphs show mean value ± SEM of 1 representative from three independent experiments (n = 3) (C) or shows pooled data from three independent experiments (n ≥ 8), p values from two-tailed t test are shown (see also Figure S2).

addition of exogenous IL-18. To determine whether IL-18 by itself was sufficient, we injected IL-18 alone or in combination with LPS into the footpad of noninfected animals. IL-18 alone was not sufficient, but required an additional TLR stimulus to induce IFNγ production by innate effectors (Figure 3B). In an attempt to further elucidate the second signal, we looked at the IFNγ response following s.c. PA infection in IL-4 KO, IL-6 KO, and IFN αβR KO mice. These mutant mice were all still able to mount a full response (data not shown), suggesting that the second signal might be redundant and supplied by several cytokines. To test this hypothesis, we coinjected IL-18 together with IL-12, IFNα, or IFNγ. Either IL-12 or IFNα was able to provide the required second signal to drive an innate lymphoid IFNγ response (Figure 3C). In contrast IFNγ was not sufficient to do so; this could be important for avoiding a feed-forward activation loop once the lymphoid cells begin to respond.

To further study the role of IL-18, LN cells were stained for IL-18R expression at steady state. Most $CD44^{hi}$ cells in the LN

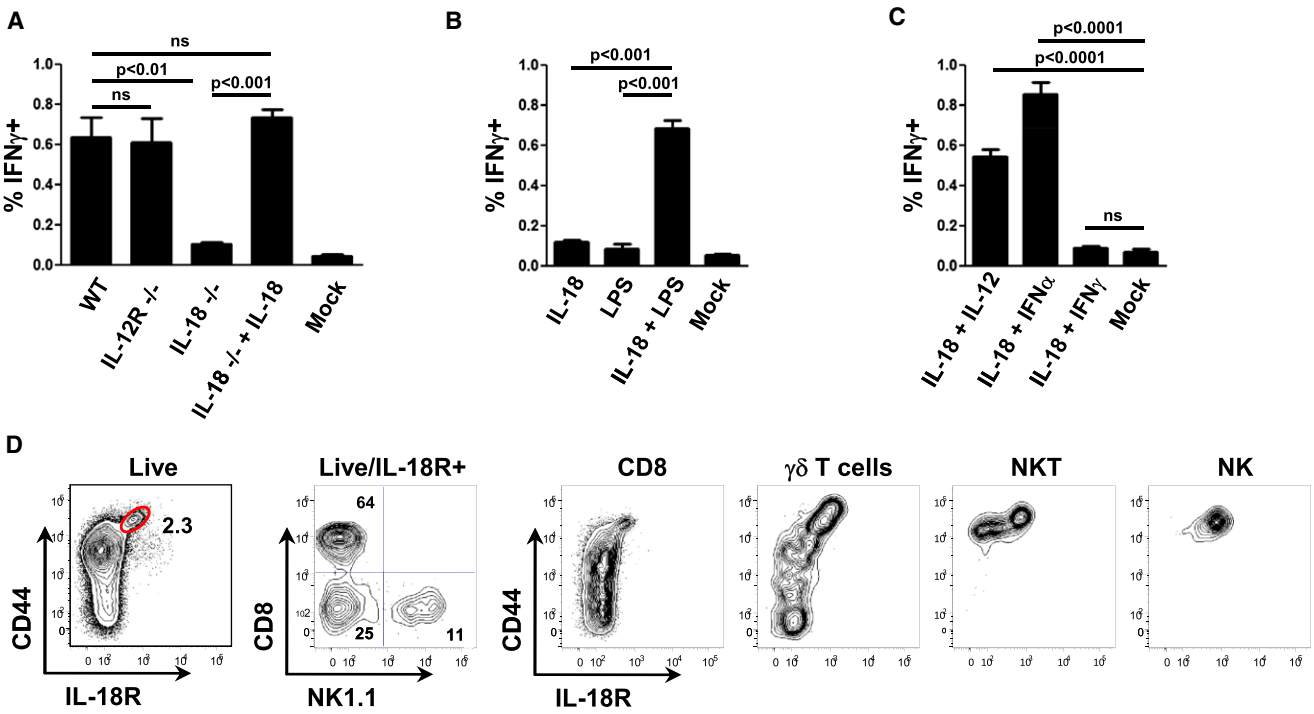

Figure 3. IL-18 Is Required, but Not Sufficient to Drive an IFNγ Response by Innate Effector Cells

(A) Intracellular IFNγ responses in cells from draining LNs 4 hr after infection with PA (±0.5 μg IL-18).

(B and C) Intracellular IFNγ responses in cells from draining LNs from noninfected WT mice 4 hr after injection with IL-18 (0.5 μg), LPS (1 μg), IL-12 (0.25 μg), IFNα (5,000 U), IFNγ (0.5 μg), or combinations thereof.

(D) Expression of IL-18R on lymphoid cell subsets in the LN. Representative flow cytometry plots of draining LNs of noninfected mice. Graphs in (A–C) show mean ± SEM from three mice per group and are representative of three similar experiments (see also Figure S3).

expressed this cytokine receptor (Figure 3D). Further subdivision of IL-18R+ cells into NK cells, γδT cells plus NKT cells, and CD8+ T cells produced a distribution quite similar to the distribution of IFNγ-producing cells after infection with PA (Figures 2D and 3D). Although all NKT cells in the LN are CD44^{hi}, only a subpopulation (NK1.1−) expresses IL-18R; in contrast all NK cells (NK1.1+) express IL-18R. Interestingly, about 9% of all CD4+/Foxp3+ (Treg) cells in the LN also express IL-18R (Figure S3). These Foxp3+ cells comprise about 10% of all CD44^{hi}/IL-18R+ cells and given the view that such Tregs are typically incapable of effector cytokine production on an acute basis (Belkaid and Tarbell, 2009), their presence can explain the small disconcordance between cells with IL-18R expression and IFNγ producers (Figure 2D and 3D).

Macrophages Have Prestored IL-18 and Release It upon Inflammasome Activation

We next set out to elucidate the pathway that leads to IL-18 production. Active IL-18 is known to derive from pro-IL-18, following cleavage that is mediated largely, but not exclusively, by caspase-1 (van de Veerdonk et al., 2011). In line with this, caspase-1 deficient mice showed a significant decrease in overall LN IFNγ-producing cells after PA challenge in the footpad (Figure 4A). Interestingly, the response from innate-like CD8+ cells was impaired, whereas the relative contribution of NK cells increased in the mutant mice (Figure 4B). IL-18R expression on NK cells is higher than on innate-like CD8+ T cells, suggesting that NK cells might be more sensitive to IL-18 and still able to respond to the lower amounts of IL-18 available in caspase-1-deficient mice (Figure 4C). In accord with this hypothesis, titration of exogenous IL-18 in the presence of LPS as a second signal showed that NK cells mediated a progressively greater proportion of the IFNγ responses as the concentration of available IL-18 and the total IFNγ response declined (Figures 4D and 4E).

To determine whether caspase-1 activation required for cleavage of pro-IL-18 to its active form is inflammasome-dependent, we analyzed the IFNγ response following s.c. infection with mutant strains of PA lacking flagellin or the type III secretion system. These virulence factors of PA activate the NLRC4 / IPAF inflammasome in vitro (Miao et al., 2008; Miao et al., 2010b). When tested in vivo, these mutant strains induced significantly reduced IFNγ responses (Figure 4F). This indicates that, at least in part, NLRC4 activation and subsequent caspase-1 cleavage initiate pro-IL-18 conversion to IL-18, which is necessary but not sufficient for initiation of the innate lymphoid effector IFNγ response.

To examine whether this IL-18 circuit directly connects SCS macrophages with the innate lymphoid populations producing the IFNγ, we looked for the cellular source of IL-18 in the LN by staining for pro-IL-18 on frozen sections. In line with our depletion studies showing macrophages as central initiators of

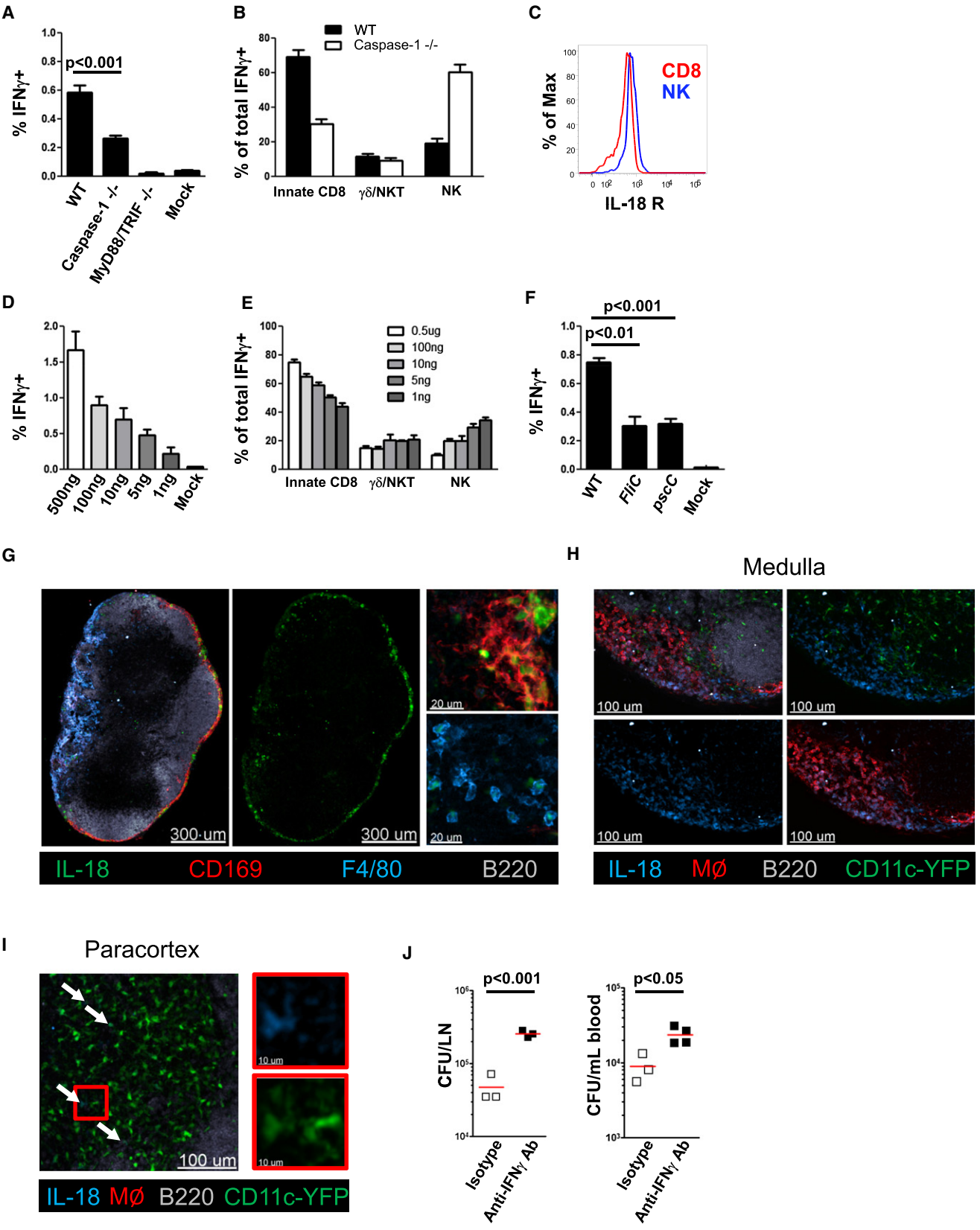
A
% IFNγ+
p<0.001
WT
Caspase-1 -/-
MyD88/TRIF -/-
Mock
B
% of total IFNγ+
WT
Caspase-1 -/-
Innate CD8
γδ/NKT
NK
C
% of Max
CD8
NK
IL-18 R
D
% IFNγ+
500ng
100ng
10ng
5ng
1ng
Mock
E
% of total IFNγ+
0.5ug
100ng
10ng
5ng
1ng
Innate CD8
γδ/NKT
NK
F
p<0.001
p<0.01
% IFNγ+
WT
FliC
pscC
Mock
G
300 um
300 um
20 um
20 um
IL-18
CD169
F4/80
B220
H
Medulla
100 um
100 um
100 um
100 um
IL-18
MØ
B220
CD11c-YFP
I
Paracortex
100 um
10 um
10 um
IL-18 MØ B220 CD11c-YFP
J
p<0.001
CFU/LN
Isotype
Anti-IFNγ Ab
p<0.05
CFU/mL blood
Isotype
Anti-IFNγ Ab

this innate response, we found abundant amounts of pro-IL-18 in SCS macrophages and in medullary macrophages of the LN under steady state conditions (Figures 4G and 4H). We could also find low intensity staining in some of CD11c+ DC in the paracortex (Figure 4I). IL-18 bright CD11c+ cells were mostly also CD169+ (Figure S4A). These cells were depleted after clodronate treatment and therefore regarded as SCS macrophages. Importantly, IL-18 staining was absent in IL-18 KO mice confirming the specificity of the staining (Figure S4B). CD8+ DCs, which have been previously suggested to be an important source of IL-18 in the spleen, did not contribute significantly to the IFNγ response in the LN after bacterial challenge (Figure S4C). Finally, to examine the functional relevance of this complex innate network, and to determine if IFNγ production contributes to pathogen control, mice were treated with IFNγ-blocking antibody or isotype control antibody prior to challenge with PA. Eight hours after infection, bacterial load in the draining LN and in the circulation was assessed. We observed a significant increase in bacterial counts in the draining LN and the blood of mice treated with IFNγ neutralizing antibody as compared to control mice (Figure 4J).

Prelocalization of Multiple Innate Lymphoid Effectors to Regions near the SCS Macrophages

Given the clodronate depletion studies and the pro-IL-18 data showing a functional link between macrophages and IFNγ-producing cells, we hypothesized that the two cellular compartments might also be spatially linked to promote the efficiency of the antipathogen response that depended on local intercellular communication between these cell populations. To examine this issue, we infected mice s.c. in the footpad with PA; harvested the dLN 4 hr later; and, after fixation, stained frozen dLN sections for the distribution of IFNγ-producing cells. Strikingly, rather than showing the central, paracortical distribution characteristic of naive T lymphocytes in an uninflamed LN, the IFNγ-producing lymphoid cells were predominantly in the medulla as well as the interfollicular zones of the organ (Figure 5A). This distribution is consistent with the data above (Figure 1D) showing a preferential accumulation of bacteria in these areas.

This static picture could have originated from either of two behaviors of the innate lymphocytes. They could reside locally at the sites of IFNγ production seen in the fixed images (either remaining largely stationary or alternatively moving within a confined microdomain), where they would be activated by macrophage-released IL-18 and a second signal. Alternatively, they could traverse large distances and volumes within the LN but become activated to produce IFN-γ when their migration brings them in close proximity to pathogen-sensing SCS macrophages and a high local concentration of IL-18. Considering the rapid onset of the IFNγ response (2 hr, Figure 2C), we questioned whether quasi-random migration would allow the innate system an opportunity for an optimally rapid response. It was thus attractive to consider that these innate effector cells might be prepositioned in the uninfected state in close proximity to the macrophages, allowing them to rapidly detect and contribute to fighting invading pathogens.

To test this hypothesis, LNs from normal uninfected mice were examined histologically for different effector cells of interest to determine their steady-state location(s). Because CD1d tetramer staining does not provide reliable results on frozen sections, we utilized the CXCR6$^{GFP/GFP}$ reporter mouse to identify NKT cells in the LNs of uninfected animals (Geissmann et al., 2005). In such knock-in mice a variety of cells express GFP to varying degrees (Unutmaz et al., 2000). Importantly, however, about 0.15% of all cells are extremely bright for GFP and all CD1d tetramer-binding NKT cells fall within this population, along with a subset of CD44^{hi} γδ T cells and an unknown population of CD4-/CD8- CD3+ cells, possibly variant NKT cells (Figure S5A). Analysis of the popliteal LN of these mice by confocal microscopy showed that GFP bright cells were located in the medulla and especially in the interfollicular region (Figure 5B). This positioning did not depend on the absence of CXCR6 in homozygous KO mice as CXCR6$^{GFP/+}$ mice showed a similar distribution (Figure S5B). In contrast to NKT cells, NK cells were predominantly found in the medulla and to a lesser extent in the interfollicular zone, but were largely absent in the deep paracortex containing the bulk of naive CD4+ and CD8+ T cells (Figure 5B). Finally, γδT cells (CD44^{hi}) were found equally in the medulla and the interfollicular zone, while also being sparse in the paracortex (Figure 5B).

Unfortunately, there is no specific marker known for the innate-like CD8+ T cells, which are the main contributors to the total IFNγ response; however, a subpopulation of these cells, like NK cells, expresses NKG2D and produces IFNγ upon PA challenge (Figures S5C and S5D). We therefore costained LNs with NKG2D, NK.1.1, CD8, and collagen IV antibodies. Again the NKG2D signal was found predominantly in the medulla of the LN, colocalizing with NK 1.1 as well as CD8 staining (Figure 5C). Thus, although there were clear differences in the preference of each innate population for particular peripheral sites, all resided in the steady state in

Figure 4. IFNγ Production by Innate Effectors Depends on Inflammasome Activation and Caspase-1 Cleavage

(A and B) Intracellular IFNγ in cells from draining LNs 4 hr after infection with PA. (A) Comparison of the frequency of IFNγ-producing cells and (B) IFNγ-producing immune cell subtypes for WT and various gene-deficient mice.

(C) Histogram showing relative IL-18R expression of NK cells and CD8^{+}/CD44^{hi} T cells.

(D and E) Intracellular IFNγ in cells from draining LNs 3 hr after noninfected WT mice were injected with graded amounts of IL-18 and LPS (1 μg). (D) Frequency of IFNγ-producing cells; (E) Immune cell subtypes producing IFNγ.

(F) Intracellular IFNγ in cells from draining LNs 4 hr after infection with WT or mutant PA lacking functional flagellin (FliC) or T3SS (pscC).

(G–I) Overview and magnified confocal IF images showing IL-18 staining in a noninfected LN from WT (G) or CD11c-YFP mice (H and I).

(J) Bacterial counts in dLN and blood of control or anti-IFNγ antibody-treated animals 8 hr after infection with PA.

Graphs (A, B, and D–F) show mean ± SEM from three mice per group and are representative of three similar experiments. MØ = combined CD169 and F4/80 staining. White arrows indicate CD11c-YFP/IL-18 double-positive cells. p values from two-tailed t test are shown (see also Figure S4).

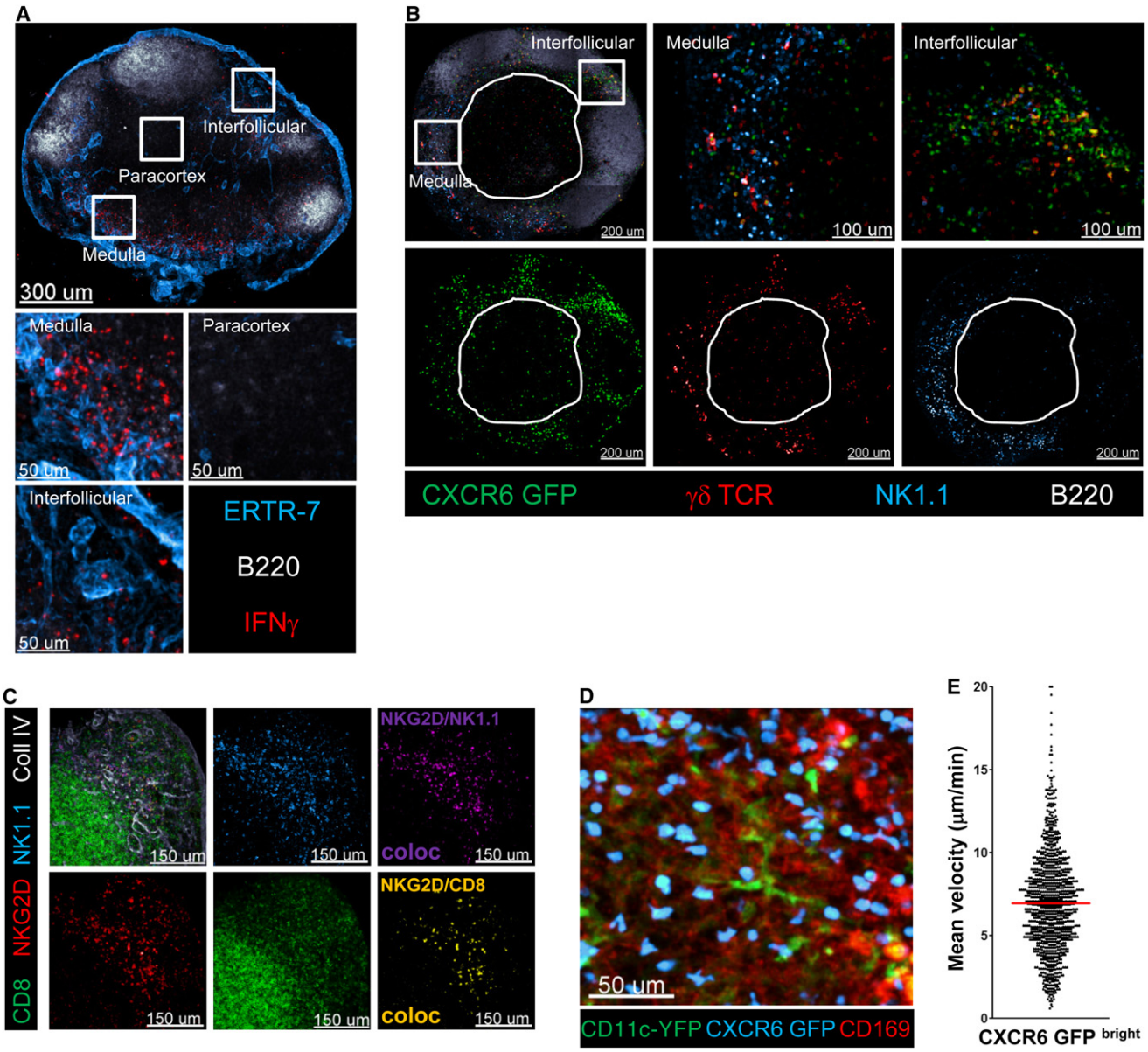

Figure 5. Innate Effector Cells Are Prepositioned in Close Proximity to LN Resident Macrophages in the Steady State

(A) Confocal IF images showing IFNγ expression in various compartments of a draining LN 4 hr after infection with PA.

(B) Confocal IF images of a popliteal LN from a noninfected CXCR6$^{gfp/gfp}$ mouse. Innate immune cell subtypes in distinct LN compartments are indicated. The white outline shows the edges of the central paracortical T cell zone.

(C) Confocal IF images of a noninfected WT LN. A colocalization channel for NKG2D/NK1.1 or NKG2D/CD8 was created to identify the localization of NK cells or innate-like CD8+ T cells, respectively.

(D) CD11c-YFP/CXCR6$^{gfp/+}$ mice were injected with labeled CD169 antibody. Image shows the maximum projection of a z stack (60 μm) from the dLN acquired in situ using a two-photon microscope.

(E) Mean velocity analysis of CXCR6-GFP^{bright} cells in situ. Data points represent individual cells from one experiment, representative of five similar experiments with mean value indicated (see also Movies S1 and S2).

confined microdomains close to the macrophages with which they communicate.

To determine the dynamic behavior of these cells, we used CXCR6$^{GFP/+}$ mice and analyzed their migratory behavior by intravital two-photon imaging. First, we tested the expectation that GFP bright cells would be localized in the periphery of the lymph node. To that end we transferred into CXCR6$^{GFP/+}$ mice a cohort of naive T cells labeled in a distinct color; these T cells home to the paracortex and roam through the dendritic cell-rich central region of the LN searching for specific antigen

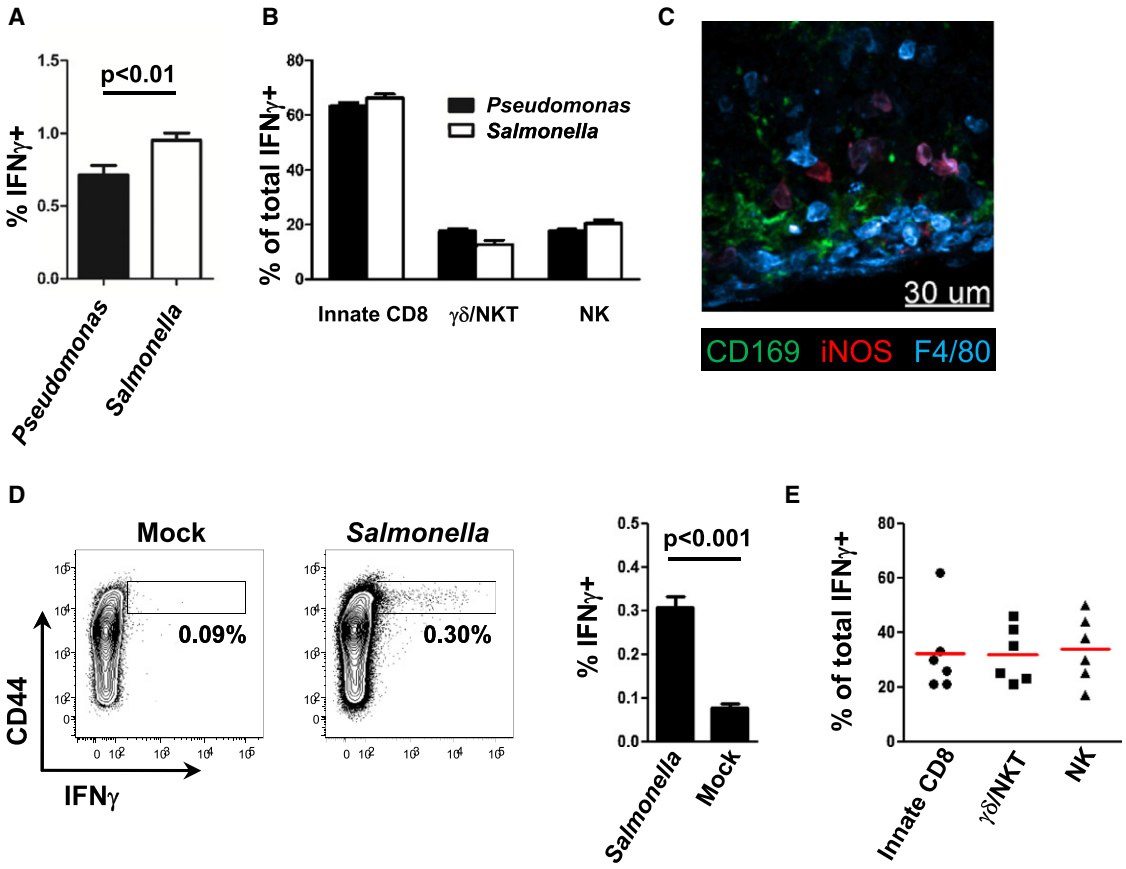

Figure 6. ST Elicits an IFNγ Response in the mLN after Oral Infection

(A and B) Intracellular IFNγ in cells from draining LNs 4 hr after s.c. infection with PA or ST. (A) Comparison of the frequency of IFNγ-producing cells and (B) IFNγ-producing immune cell subtypes.

(C) Confocal IF image for iNOS localization in a draining LN 8 hr after infection with ST.

(D and E) Analysis of intracellular IFNγ in cells from mLNs 48 hr after oral infection with ST. (D) Comparison of the frequency of IFNγ-producing cells and (E) IFNγ-producing immune cell subtypes. Graphs show mean ± SEM from six mice per group and are representative of two similar experiments. p values from two-tailed t test are shown (see also Figure S5).

(Movie S1), providing a control population of known location and migratory behavior in our imaging studies. In line with our static imaging data (Figure 5B), we found CXCR6-GFP^{bright} cells to be located close to the capsule in the interfollicular area, although being almost absent in the paracortex where we could easily detect naive CD8+ T cells. To further examine the proximity of the CXCR6-GFP^{bright} cells to the subcapsular sinus macrophages, we injected labeled anti-CD169 antibody into CXCR6$^{GFP/+}$/CD11c-YFP mice and confirmed the spatial connection between these cell populations (Figure 5D). The CXCR6 GFP^{hi} cells moved at an average speed of about 7 μm/min in close proximity to the labeled CD169+ SCS macrophages (Figure 5E and Movie S2). From these data, we conclude that various innate effector cells are strategically prepositioned in a nonrandom fashion within subregions of the LN, in particular in the interfollicular zones and the medulla. They actively scan these areas near to resident macrophages, which provide IL-18 and possibly a second cytokine signal that are together required to activate the local innate lymphocyte populations upon acute infection.

Oral Infection with Salmonella Induces Innate IFNγ Responses in the Draining LNs

PA has evolved mechanisms to counteract the action of IFNγ by direct sensing of the cytokine and subsequent upregulation of virulence factors (Wu et al., 2005). We were therefore interested in determining whether intracellular bacteria, for instance *Salmonella typhimurium* (ST) with a well-documented greater sensitivity toward IFNγ, would elicit a similar response. To examine this issue, ST was injected into the footpad of mice and the IFNγ response in dLNs was analyzed 4 hr later. The magnitude of IFNγ production was significantly elevated, but the cellular composition of the IFNγ-producing cells was largely similar to that seen after PA infection by the same route (Figures 6A and 6B). Furthermore, after footpad infection with ST we could clearly detect iNOS+ macrophages in the dLN, an indication of a local feedback effect of the IL-18-elicited IFNγ on the myeloid cells that first started this acute response (Figures 6C and S6A). Because the natural route of infection of ST is oral, we also analyzed the draining mesenteric LN (mLN) for IFNγ production after bacterial gavage. Two days after oral infection

with ST there was a significant IFNγ response in the draining mLNs (Figure 6D). The cellular composition of the IFNγ-producing cells was more variable than seen after skin infection (Figure 6E), in line with our data suggesting a different sensitivity of the various innate cells toward IL-18 (Figure 4E) and with a less synchronized infection of the mLN after oral administration as opposed to the skin dLN after footpad injection. Importantly, we also observed a similar geographic prepositioning of the various lymphoid effectors in the mLN (Figure S6B). These findings indicate that this newly elucidated structural and functional prepositioning of cells in the lymph node, and its role in promoting acute host defense responses has significance in the context of different classes of pathogens and throughout the body.

Neutrophils Are Recruited to dLNs by an Inflammasome-Dependent Mechanism Involving SCS Macrophages

Neutrophils play a dominant role in protection against pathogen invasion, particularly extracellular bacteria. Therefore, we examined whether these myeloid cells were also involved in the layered innate defense network of the LN. As a first test of the possible role of neutrophils in controlling pathogen spread within dLNs after skin infection, we treated mice with Ly6G depleting antibody or isotype control antibody prior to s.c. challenge with PA. Eight hours after infection, the bacterial load in the draining LN was assessed. There was a significant increase in bacterial counts in the dLN and in the blood of neutrophil-depleted mice as compared to control mice (Figure 7A). At steady-state neutrophils are largely absent from the LN parenchyma. However, 4 hr after infection with PA, we found strong recruitment of neutrophils to the subcapsular, medullary, and interfollicular areas of the dLN (Figure 7B), mirroring the distribution of the innate immune lymphocytes communicating with SCS macrophages. There was an average of about 8 × 10^3 neutrophils in the draining popliteal LN (Figure 7C), representing ~2%–3% of the total hematopoietic cell population. This neutrophil recruitment, like the activation of innate lymphoid effector cells, depended substantially on the presence of macrophages in the LN (Figure 7C). Therefore, we hypothesized that, like innate cell activation, neutrophil recruitment to the LN might be dependent on inflammasome-mediated activation of macrophages and caspase-1-dependent cytokine production, in this case more likely on production of IL-1 rather than IL-18 (Miller et al., 2007; Moayeri et al., 2010). To test this idea, we compared neutrophil recruitment in wild-type (WT) and IL-1R KO mice and, as predicted, found a significant reduction in neutrophil recruitment in IL-1R KO mice (Figure 7D). Notably, IL-1β is not expressed under noninflammatory conditions, but 2 hr after infection, we were able to detect a strong IL-1β signal in both macrophages and dendritic cells (Figure 7E and 7F). This IL-1β expression outlined the medullary and interfollicular areas, the same regions that harbor the innate lymphocytes (Figure 5B), function as entry portals for lymph-borne pathogens (Figure 1D), and where pro-IL-18 is found in steady-state LNs (Figure 4G). Although both PA and ST can cause pyroptosis of macrophages, ST has developed mechanisms to eventually survive within and prevent pyroptosis of macrophages. In line with the described IL-1β production and the known biology of ST, neutrophil recruitment after ST infection was significantly lower than after PA infection (Figure 7G and 7H), suggesting that such recruitment may play a more crucial role in the response to extracellular (PA) as compared to intracellular (ST) pathogens.

DISCUSSION

Our findings reveal a geographically-delimited, multiplex cellular organization of the LN that plays a key role in orchestrating cytokine-dependent acute innate immune responses against both intra- and extracellular pathogens arriving via the lymph. LN-resident macrophages serve as the first line of defense to prevent systemic spread of such lymph-borne pathogens. They achieve this goal initially by sequestering pathogens as they enter the SCS in the afferent lymph as previously described (Junt et al., 2007), thus limiting passage into the efferent lymph and the blood circulation. We now show that these macrophages also activate innate lymphoid cells to produce cytokines such as IFNγ that enhance the antimicrobial activity of the phagocytes, thus reciprocally contributing to more effective host defense. The co-operating lymphoid cells are not randomly dispersed throughout the LN but are strategically prepositioned in the uninfected host in close physical proximity to the macrophages and actively migrate near the macrophage layer. Microbial resistance is further augmented by macrophage-mediated recruitment of neutrophils. The operation of this complex cellular network depends on activation of one or more NLR-based inflammasomes in the pathogen-sensing macrophages that generate active IL-1β and IL-18; the former promotes neutrophil recruitment to handle extracellular bacteria, and the latter, via IFNγ induction, plays a specific role in eliminating intracellular or engulfed bacteria. Taken together, these new findings redefine our current understanding of the functional and spatial organization of the lymph node, emphasize that the LN is a primary site of host defense rather than just a staging area for generation of adaptive effector cells that disperse into infected tissues and reveal how anatomy combines with intercellular communication via molecular networks to promote innate host defense against lymph-borne pathogens (Figure S7).

For lymphocytes with clonal (T cells) or quasi-clonal (NK cells) recognition receptors, there is a need for extensive migration to bring rare members of these populations in contact with their specific ligands, which are often associated with other hematopoietic cell types in those organs. In this context the present findings of a precise preorganization of innate lymphoid cells in the LN, spatially poised to receive messages from and transmit signals back to the sentinel macrophages that receive afferent lymph flow, provide significant insight into how evolution has solved this problem. A delay in evoking innate responses places the host at increased risk; therefore, extensive migration of innate lymphoid cells throughout a large tissue volume away from the macrophages poised for direct sensing of invading pathogens would be deleterious and prepositioning the innate lymphocytes near to the entry site of invading pathogens solves this problem. A similar principle of effector localization near anticipated sites of pathogen entry is seen in peripheral tissues after an adaptive immune response has been mounted (Clark et al., 2006; Gebhardt et al., 2009; Wakim et al., 2010). It remains

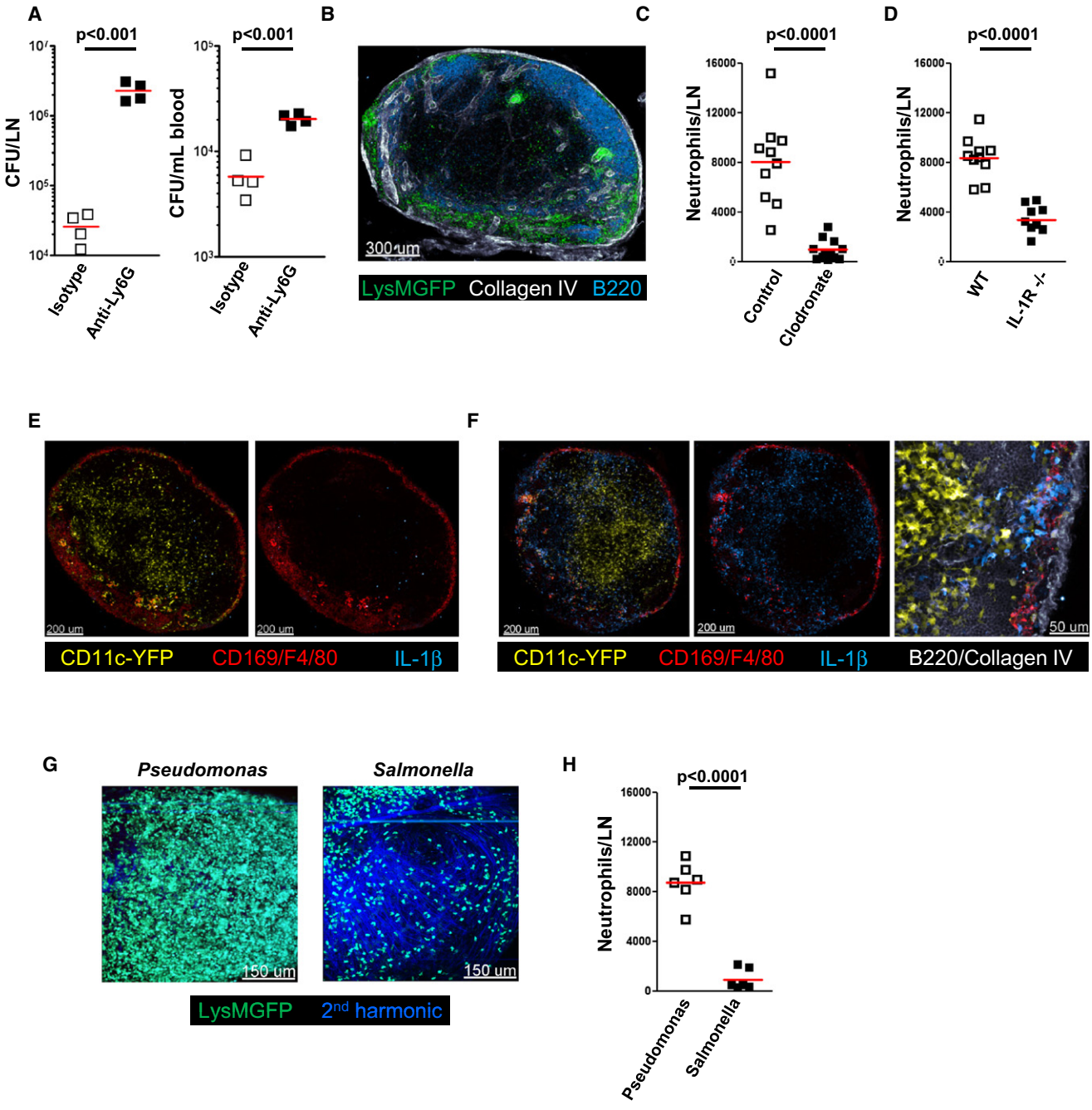

Figure 7. Macrophages produce IL-1 that recruits neutrophils to the LN

(A) Effect of neutrophil depletion on bacterial counts in blood and dLN 8 hr after s.c. infection with PA. Mice were pretreated with isotype control or anti-Ly6G antibody 24 hr before infection.

(B) Confocal IF image of draining LN from LysM$^{gfp/gfp}$ mice 4 hr after s.c. infection with PA.

(C) Flow cytometric analysis of neutrophil (CD11b+/Ly6G+) numbers in draining LN 4 hr after s.c. infection with PA. WT mice were pretreated 7 days before infection with control or clodronate-containing liposomes.

(D) Flow cytometric analysis of neutrophil (CD11b+/Ly6G+) numbers in the draining LN of WT and IL-1R KO mice 4 hr after s.c. infection with PA.

(E and F) Confocal IF images of IL-1β localization in dLN of noninfected (E) or PA infected (2 hr) (F) CD11c-YFP mice.

(G) LysM$^{gfp/gfp}$ mice were infected with PA or ST for 4 hr. Images show the maximum projection of a z stack (90 μm) from the dLN acquired in situ using a 2-photon microscope.

(H) Analysis of neutrophil (CD11b+/Ly6G+) numbers in dLN of WT mice 4 hr after s.c. infection with PA or ST.

Data are representative of three independent experiments (A and H) or shows pooled data from three independent experiments (C and D). Bars show mean values. p values from two-tailed t test are shown.

unclear what factors orchestrate the positioning of such tissue resident memory CD8+ T cells or the various innate lymphoid cells in the LN (Bajénoff et al., 2006a).

In distinction to the result reported here, a previous study reported antigen-specific priming of iNKT cells by SCS macrophages (Barral et al., 2010). In these experiments, donor cells derived from the liver, spleen, and LN of TCR transgenic mice were employed and after transfer these cells were primarily localized to the paracortex, intermixed with naive T cells known to migrate within that region of the LN. The iNKT cells only occasionally migrated to the SCS for interaction with macrophages in that peripheral zone of the tissue. The specific basis for the differences between our findings on in situ cell distribution of NKT and these results with transferred iNKT cells is unknown. However, we have noted in numerous transfer experiments with various $CD44^{hi}$ cell populations that their distribution in the LN does not match that of what are phenotypically the same cell populations analyzed directly in the tissue, suggesting the possibility of alterations in homing properties induced by the manipulations involved in isolation, purification, and transfer.

Beyond documenting the unexpected spatial organization of innate lymphoid cells in the LN, our study has also has revealed the molecular basis for communication between the gatekeeper macrophages and these lymphoid cells, namely IL-18 and several complementary cytokines that together elicit an IFNγ response. The NLRC4 inflammasome appears to be the major sensing pathway for PA leading to production of active IL-18 (Sutterwala et al., 2007). Downstream of NLR pathogen sensing is caspase-1 activation, which in turn acts on pro-IL-18 that we show here is present in the LN-resident macrophages in the uninfected state. This is different from the conventional model that presumes a requirement for a "priming" step that induces transcription and translation of the proform of this molecule prior to its activation by enzymatic cleavage (van de Veerdonk et al., 2011). We could detect an innate IFNγ response after MVA infection, albeit at a significantly lower level than we saw using PA. However, we were unable to measure such responses after VV infection of the skin. This suggests that viruses have evolved mechanisms to evade this innate inflammasome-driven response. Indeed, VV expresses a plethora of proteins to counteract this system, ranging from caspase-1 inhibitors to IL-18-, IFNα-, and IFNγ-binding proteins, which contribute to its virulence (Kettle et al., 1997; Symons et al., 2002).

The flip side of an immediate IL-18 response from preformed pro-IL-18 is the danger posed by an overexuberant response. To prevent this outcome, we found the IFNγ response to have a requirement for a second complementing cytokine. A recent report claimed that an IL-18 signal by itself is sufficient to induce an IFNγ response by noncognate memory CD8+ T cells in the spleen (Kupz et al., 2012). However, that study used a supraphysiological amount of IL-18 to induce this response and in our hands as little as 10 ng, rather than the 1,000-fold more used previously, were sufficient to drive a robust response in the presence of LPS (Figure 4D). This suggests that the very high amounts used in this prior study may have obscured the usual requirement for a complementary signal.

A surprising result was the significant contribution of innate-like CD8+ cells to the total early IFNγ response after bacterial infection. NKT/IL-4-dependent innate CD8+ T cells have been described in Balb/c mice (Weinreich et al., 2010) but are largely absent in B6 mice, and in our experiments neither IL-4 nor NKT cells were required for the development or function of innate-like CD8+ T cells. Instead, these cells appear most like naive CD8+ T cells that proliferate in relatively lymphopenic neonatal animals, acquiring memory/effector functions (Lee et al., 2011).

The innate defense system in the LN described here does not appear to fully discriminate between extra- and intracellular pathogens. Rather, several effector mechanisms and effector cells are recruited and/or activated together. This may relate to how bacterial pathogens attempt to evade host defenses. Intracellular pathogens like ST downregulate flagellin expression upon infection of macrophages, thereby limiting sensing by the inflammasome and subsequent pyroptosis, and forced expression of flagellin in ST significantly attenuates its virulence (Miao et al., 2010a). As in the case of ST, the innate IFNγ response is particularly important to help fight pathogens that evade pyroptosis and remain inside the cell.

Relating structure to function is an essential part of investigation at all biological scales, from the molecular to the organismal. Here we have revealed a new aspect of lymphoid tissue architecture that involves local residence of a series of innate lymphoid cells near to peripherally distributed macrophages that serve as gatekeepers sensing pathogens arriving in the afferent lymph. Through a series of reciprocal cytokine-mediated communication channels, these spatially constrained cell populations provide a rapid response to organisms hitchhiking in the lymphatic flow, preventing their systemic dissemination. This description alters our classical view of LNs as only sites within which adaptive immunity develops by revealing the composition, organization, and operation of a robust and functionally critical active innate defense apparatus within these secondary lymphoid organs.

EXPERIMENTAL PROCEDURES

Mice

Mice were purchased from Jackson Laboratories or were kindly provided or obtained from Taconic Laboratories through a special contract with the NIAID (for details see Supplemental Information). All mice were maintained in specific-pathogen-free conditions at an Association for Assessment and Accreditation of Laboratory Animal Care-accredited animal facility at the NIAID. All procedures were approved by the NIAID animal care and use committee (National Institutes of Health, Bethesda, MD).

Bacterial and Viral Infections

MVA (pH5) GFP was constructed as previously described using pLW-73 (Kastenmuller et al., 2007; Wyatt et al., 2009); 10^8 infectious units (IU) vaccinia virus (MVA) or 10^7 colony-forming units (CFU) *Pseudomonas aeroguinosa* GFP, WT, FliC mutant, pscC mutant or ST (SL1344) were diluted in PBS and injected in the footpad (30 μl) (Davies et al., 1998; Miao et al., 2008; Miao et al., 2010b). For oral infections, 10^9 CFU ST diluted in 500 μl PBS was applied orally using a gavage needle.

In Vivo Depletion of LN Macrophages

For in vivo depletion of LN macrophages, mice were injected in the footpad or the calf with 20 μl or 30 μl of clodronate containing liposomes or empty liposomes as control (Encapsula) 7 days before infection. Clodronate injection did not lead to granuloma formation at the site of injection or to enlargement of the depleted LN.

Flow Cytometry

For analysis of intracellular cytokine production, preparation of cell suspensions from draining lymph nodes and subsequent staining was done in the presence of (1 μg/ml) brefeldin A (Sigma). Flow cytometric data were collected on an LSR II (BD Biosciences) and analyzed with FlowJo software (TreeStar). For details on antibodies see Supplemental Information.

Immunofluorescence Staining

Lymph nodes and spleens were harvested and fixed by using paraformaldehyde/lysine/periodate (PLP) buffer for 12 hr, then dehydrated in 30% sucrose prior to embedding in OCT-freezing media (Sakura Finetek). Serial lymph node sections were prepared (30 μm), permeabilized (Triton X-100), and blocked with 10% normal mouse serum (Jackson Immunoresearch). Stained slides were mounted (Southern Biotech), each section was visually inspected and several representative sections were acquired on a 710 confocal microscope (Carl Zeiss Microimaging). For details on antibodies see Supplemental Information.

Intravital Two-Photon Imaging

Mice were anesthetized with isoflurane, popliteal LNs were exposed, and intravital microscopy was performed using a protocol modified from a previous report (Bajénoff et al., 2006b). For static imaging our field was typically a z stack reaching from the capsule to 200 μm below and using 1 μm steps. For dynamic imaging, we used a z stack of 90 μm and 3 μm step size or 60 μm and 2 μm step size and acquired every 40 s. Raw imaging data were processed and analyzed with Imaris (Bitplane).

Statistical Analysis

Student's t test (two-tailed) and Mann-Whitney test were used for the statistical analysis of differences between two groups with normal or nonnormal distribution, respectively.

SUPPLEMENTAL INFORMATION

Supplemental Information includes Extended Experimental Procedures, seven figures, and two movies and can be found with this article online at http://dx.doi.org/10.1016/j.cell.2012.07.021.

ACKNOWLEDGMENTS

This research was supported by the Intramural Research Program, NIAID, NIH, DFG, KA 3091/1-1 to W.K. and by a fellowship grant from the International Human Frontier Science Program to T.L. We thank A. Sher, Y. Belkaid, and K. Abdi for kindly providing mouse strains, B. Moss for generously providing pLW-73, E. Miao and B. Borlee for generously providing PA strains and E. Long for critically reading this manuscript. The authors would also like to thank Austin Rinker for technical support.

Received: February 22, 2012
Revised: May 9, 2012
Accepted: July 24, 2012
Published: September 13, 2012

REFERENCES

Alitalo, K. (2011). The lymphatic vasculature in disease. Nat. Med. *17*, 1371–1380.

Asano, K., Nabeyama, A., Miyake, Y., Qiu, C.H., Kurita, A., Tomura, M., Kanagawa, O., Fujii, S., and Tanaka, M. (2011). CD169-positive macrophages dominate antitumor immunity by crosspresenting dead cell-associated antigens. Immunity *34*, 85–95.

Bajénoff, M., Breart, B., Huang, A.Y., Qi, H., Cazareth, J., Braud, V.M., Germain, R.N., and Glaichenhaus, N. (2006a). Natural killer cell behavior in lymph nodes revealed by static and real-time imaging. J. Exp. Med. *203*, 619–631.

Bajénoff, M., Egen, J.G., Koo, L.Y., Laugier, J.P., Brau, F., Glaichenhaus, N., and Germain, R.N. (2006b). Stromal cell networks regulate lymphocyte entry, migration, and territoriality in lymph nodes. Immunity *25*, 989–1001.

Barral, P., Polzella, P., Bruckbauer, A., van Rooijen, N., Besra, G.S., Cerundolo, V., and Batista, F.D. (2010). CD169(+) macrophages present lipid antigens to mediate early activation of iNKT cells in lymph nodes. Nat. Immunol. *11*, 303–312.

Belkaid, Y., and Tarbell, K. (2009). Regulatory T cells in the control of host-microorganism interactions. Annu. Rev. Immunol. *27*, 551–589.

Bendelac, A., Savage, P.B., and Teyton, L. (2007). The biology of NKT cells. Annu. Rev. Immunol. *25*, 297–336.

Benoit, M., Desnues, B., and Mege, J.L. (2008). Macrophage polarization in bacterial infections. J. Immunol. *181*, 3733–3739.

Bodey, G.P., Bolivar, R., Fainstein, V., and Jadeja, L. (1983). Infections caused by Pseudomonas aeruginosa. Rev. Infect. Dis. *5*, 279–313.

Borrow, P., Lewicki, H., Wei, X., Horwitz, M.S., Peffer, N., Meyers, H., Nelson, J.A., Gairin, J.E., Hahn, B.H., Oldstone, M.B., and Shaw, G.M. (1997). Antiviral pressure exerted by HIV-1-specific cytotoxic T lymphocytes (CTLs) during primary infection demonstrated by rapid selection of CTL escape virus. Nat. Med. *3*, 205–211.

Cahalan, M.D., and Parker, I. (2006). Imaging the choreography of lymphocyte trafficking and the immune response. Curr. Opin. Immunol. *18*, 476–482.

Carrasco, Y.R., and Batista, F.D. (2007). B cells acquire particulate antigen in a macrophage-rich area at the boundary between the follicle and the subcapsular sinus of the lymph node. Immunity *27*, 160–171.

Castellino, F., Huang, A.Y., Altan-Bonnet, G., Stoll, S., Scheinecker, C., and Germain, R.N. (2006). Chemokines enhance immunity by guiding naive CD8+ T cells to sites of CD4+ T cell-dendritic cell interaction. Nature *440*, 890–895.

Chtanova, T., Schaeffer, M., Han, S.J., van Dooren, G.G., Nollmann, M., Herzmark, P., Chan, S.W., Satija, H., Camfield, K., Aaron, H., et al. (2008). Dynamics of neutrophil migration in lymph nodes during infection. Immunity *29*, 487–496.

Cinamon, G., Zachariah, M.A., Lam, O.M., Foss, F.W., Jr., and Cyster, J.G. (2008). Follicular shuttling of marginal zone B cells facilitates antigen transport. Nat. Immunol. *9*, 54–62.

Clark, R.A., Chong, B., Mirchandani, N., Brinster, N.K., Yamanaka, K., Dowgiert, R.K., and Kupper, T.S. (2006). The vast majority of CLA+ T cells are resident in normal skin. J. Immunol. *176*, 4431–4439.

Davies, D.G., Parsek, M.R., Pearson, J.P., Iglewski, B.H., Costerton, J.W., and Greenberg, E.P. (1998). The involvement of cell-to-cell signals in the development of a bacterial biofilm. Science *280*, 295–298.

Dayer, J.M. (2003). How T-lymphocytes are activated and become activators by cell-cell interaction. Eur. Respir. J. Suppl. *44*, 10s–15s.

DeGrendele, H.C., Estess, P., and Siegelman, M.H. (1997). Requirement for CD44 in activated T cell extravasation into an inflammatory site. Science *278*, 672–675.

Gebhardt, T., Wakim, L.M., Eidsmo, L., Reading, P.C., Heath, W.R., and Carbone, F.R. (2009). Memory T cells in nonlymphoid tissue that provide enhanced local immunity during infection with herpes simplex virus. Nat. Immunol. *10*, 524–530.

Geissmann, F., Cameron, T.O., Sidobre, S., Manlongat, N., Kronenberg, M., Briskin, M.J., Dustin, M.L., and Littman, D.R. (2005). Intravascular immune surveillance by CXCR6+ NKT cells patrolling liver sinusoids. PLoS Biol. *3*, e113.

Germain, R.N., Bajénoff, M., Castellino, F., Chieppa, M., Egen, J.G., Huang, A.Y., Ishii, M., Koo, L.Y., and Qi, H. (2008). Making friends in out-of-the-way places: how cells of the immune system get together and how they conduct their business as revealed by intravital imaging. Immunol. Rev. *221*, 163–181.

Gonzalez, S.F., Lukacs-Kornek, V., Kuligowski, M.P., Pitcher, L.A., Degn, S.E., Kim, Y.A., Cloninger, M.J., Martinez-Pomares, L., Gordon, S., Turley, S.J., and Carroll, M.C. (2010). Capture of influenza by medullary dendritic cells via SIGN-R1 is essential for humoral immunity in draining lymph nodes. Nat. Immunol. *11*, 427–434.

Gretz, J.E., Anderson, A.O., and Shaw, S. (1997). Cords, channels, corridors and conduits: critical architectural elements facilitating cell interactions in the lymph node cortex. Immunol. Rev. *156*, 11–24.

Guo, L., Wei, G., Zhu, J., Liao, W., Leonard, W.J., Zhao, K., and Paul, W. (2009). IL-1 family members and STAT activators induce cytokine production by Th2, Th17, and Th1 cells. Proc. Natl. Acad. Sci. USA *106*, 13463–13468.

Hayday, A.C. (2009). Gammadelta T cells and the lymphoid stress-surveillance response. Immunity *31*, 184–196.

Junt, T., Moseman, E.A., Iannacone, M., Massberg, S., Lang, P.A., Boes, M., Fink, K., Henrickson, S.E., Shayakhmetov, D.M., Di Paolo, N.C., et al. (2007). Subcapsular sinus macrophages in lymph nodes clear lymph-borne viruses and present them to antiviral B cells. Nature *450*, 110–114.

Kastenmuller, W., Gasteiger, G., Gronau, J.H., Baier, R., Ljapoci, R., Busch, D.H., and Drexler, I. (2007). Cross-competition of CD8+ T cells shapes the immunodominance hierarchy during boost vaccination. J. Exp. Med. *204*, 2187–2198.

Kastenmüller, W., Gerner, M.Y., and Germain, R.N. (2010). The in situ dynamics of dendritic cell interactions. Eur. J. Immunol. *40*, 2103–2106.

Kettle, S., Alcamí, A., Khanna, A., Ehret, R., Jassoy, C., and Smith, G.L. (1997). Vaccinia virus serpin B13R (SPI-2) inhibits interleukin-1beta-converting enzyme and protects virus-infected cells from TNF- and Fas-mediated apoptosis, but does not prevent IL-1beta-induced fever. J. Gen. Virol. *78*, 677–685.

Kupz, A., Guarda, G., Gebhardt, T., Sander, L.E., Short, K.R., Diavatopoulos, D.A., Wijburg, O.L., Cao, H., Waithman, J.C., Chen, W., et al. (2012). NLRC4 inflammasomes in dendritic cells regulate noncognate effector function by memory CD8$^+$ T cells. Nat. Immunol. *13*, 162–169.

Lämmermann, T., and Sixt, M. (2008). The microanatomy of T-cell responses. Immunol. Rev. *221*, 26–43.

Lee, Y.J., Jameson, S.C., and Hogquist, K.A. (2011). Alternative memory in the CD8 T cell lineage. Trends Immunol. *32*, 50–56.

Mantovani, A., Sozzani, S., Locati, M., Allavena, P., and Sica, A. (2002). Macrophage polarization: tumor-associated macrophages as a paradigm for polarized M2 mononuclear phagocytes. Trends Immunol. *23*, 549–555.

Miao, E.A., Ernst, R.K., Dors, M., Mao, D.P., and Aderem, A. (2008). Pseudomonas aeruginosa activates caspase 1 through Ipaf. Proc. Natl. Acad. Sci. USA *105*, 2562–2567.

Miao, E.A., Leaf, I.A., Treuting, P.M., Mao, D.P., Dors, M., Sarkar, A., Warren, S.E., Wewers, M.D., and Aderem, A. (2010a). Caspase-1-induced pyroptosis is an innate immune effector mechanism against intracellular bacteria. Nat. Immunol. *11*, 1136–1142.

Miao, E.A., Mao, D.P., Yudkovsky, N., Bonneau, R., Lorang, C.G., Warren, S.E., Leaf, I.A., and Aderem, A. (2010b). Innate immune detection of the type III secretion apparatus through the NLRC4 inflammasome. Proc. Natl. Acad. Sci. USA *107*, 3076–3080.

Miller, L.S., Pietras, E.M., Uricchio, L.H., Hirano, K., Rao, S., Lin, H., O'Connell, R.M., Iwakura, Y., Cheung, A.L., Cheng, G., and Modlin, R.L. (2007). Inflammasome-mediated production of IL-1beta is required for neutrophil recruitment against Staphylococcus aureus in vivo. J. Immunol. *179*, 6933–6942.

Moayeri, M., Crown, D., Newman, Z.L., Okugawa, S., Eckhaus, M., Cataisson, C., Liu, S., Sastalla, I., and Leppla, S.H. (2010). Inflammasome sensor Nlrp1b-dependent resistance to anthrax is mediated by caspase-1, IL-1 signaling and neutrophil recruitment. PLoS Pathog. *6*, e1001222.

Norbury, C.C., Malide, D., Gibbs, J.S., Bennink, J.R., and Yewdell, J.W. (2002). Visualizing priming of virus-specific CD8+ T cells by infected dendritic cells in vivo. Nat. Immunol. *3*, 265–271.

Okada, T., and Cyster, J.G. (2006). B cell migration and interactions in the early phase of antibody responses. Curr. Opin. Immunol. *18*, 278–285.

Pereira, J.P., Kelly, L.M., and Cyster, J.G. (2010). Finding the right niche: B-cell migration in the early phases of T-dependent antibody responses. Int. Immunol. *22*, 413–419.

Robinson, D., Shibuya, K., Mui, A., Zonin, F., Murphy, E., Sana, T., Hartley, S.B., Menon, S., Kastelein, R., Bazan, F., and O'Garra, A. (1997). IGIF does not drive Th1 development but synergizes with IL-12 for interferon-gamma production and activates IRAK and NFkappaB. Immunity *7*, 571–581.

Senkevich, T.G., Wolffe, E.J., and Buller, R.M. (1995). Ectromelia virus RING finger protein is localized in virus factories and is required for virus replication in macrophages. J. Virol. *69*, 4103–4111.

Shi, F.D., Ljunggren, H.G., La Cava, A., and Van Kaer, L. (2011). Organ-specific features of natural killer cells. Nat. Rev. Immunol. *11*, 658–671.

Sumen, C., Mempel, T.R., Mazo, I.B., and von Andrian, U.H. (2004). Intravital microscopy: visualizing immunity in context. Immunity *21*, 315–329.

Sutterwala, F.S., Mijares, L.A., Li, L., Ogura, Y., Kazmierczak, B.I., and Flavell, R.A. (2007). Immune recognition of Pseudomonas aeruginosa mediated by the IPAF/NLRC4 inflammasome. J. Exp. Med. *204*, 3235–3245.

Swartz, M.A. (2001). The physiology of the lymphatic system. Adv. Drug Deliv. Rev. *50*, 3–20.

Symons, J.A., Adams, E., Tscharke, D.C., Reading, P.C., Waldmann, H., and Smith, G.L. (2002). The vaccinia virus C12L protein inhibits mouse IL-18 and promotes virus virulence in the murine intranasal model. J. Gen. Virol. *83*, 2833–2844.

Unutmaz, D., Xiang, W., Sunshine, M.J., Campbell, J., Butcher, E., and Littman, D.R. (2000). The primate lentiviral receptor Bonzo/STRL33 is coordinately regulated with CCR5 and its expression pattern is conserved between human and mouse. J. Immunol. *165*, 3284–3292.

van de Veerdonk, F.L., Netea, M.G., Dinarello, C.A., and Joosten, L.A. (2011). Inflammasome activation and IL-1β and IL-18 processing during infection. Trends Immunol. *32*, 110–116.

Van Rooijen, N., and Sanders, A. (1994). Liposome mediated depletion of macrophages: mechanism of action, preparation of liposomes and applications. J. Immunol. Methods *174*, 83–93.

Wakim, L.M., Woodward-Davis, A., and Bevan, M.J. (2010). Memory T cells persisting within the brain after local infection show functional adaptations to their tissue of residence. Proc. Natl. Acad. Sci. USA *107*, 17872–17879.

Weinreich, M.A., Odumade, O.A., Jameson, S.C., and Hogquist, K.A. (2010). T cells expressing the transcription factor PLZF regulate the development of memory-like CD8+ T cells. Nat. Immunol. *11*, 709–716.

Wu, L., Estrada, O., Zaborina, O., Bains, M., Shen, L., Kohler, J.E., Patel, N., Musch, M.W., Chang, E.B., Fu, Y.X., et al. (2005). Recognition of host immune activation by Pseudomonas aeruginosa. Science *309*, 774–777.

Wyatt, L.S., Earl, P.L., Xiao, W., Americo, J.L., Cotter, C.A., Vogt, J., and Moss, B. (2009). Elucidating and minimizing the loss by recombinant vaccinia virus of human immunodeficiency virus gene expression resulting from spontaneous mutations and positive selection. J. Virol. *83*, 7176–7184.

Yang, J., Zhu, H., Murphy, T.L., Ouyang, W., and Murphy, K.M. (2001). IL-18-stimulated GADD45 beta required in cytokine-induced, but not TCR-induced, IFN-gamma production. Nat. Immunol. *2*, 157–164.